Science Advances
AAAS

advances.sciencemag.org/cgi/content/full/5/9/eaax1874/DC1

Supplementary Materials for

Simulation of Eocene extreme warmth and high climate sensitivity through cloud feedbacks

Jiang Zhu*, Christopher J. Poulsen, Jessica E. Tierney

*Corresponding author. Email: jiazhu@umich.edu

Published 18 September 2019, *Sci. Adv.* **5**, eaax1874 (2019)
DOI: 10.1126/sciadv.aax1874

The PDF file includes:

Other Supplementary Material for this manuscript includes the following:

(available at advances.sciencemag.org/cgi/content/full/5/9/eaax1874/DC1)

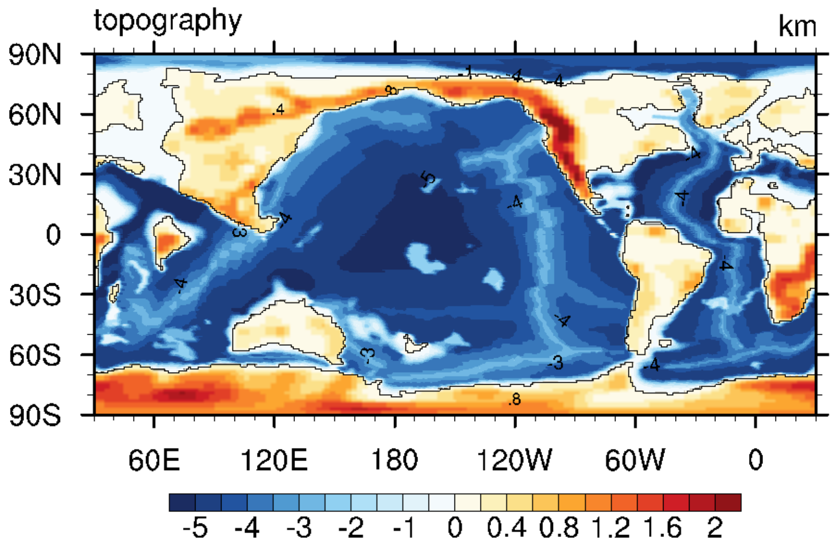

Fig. S1. Topography and bathymetry at model resolution. Topography and bathymetry (in km) are generated from Herold et al. (*39*).

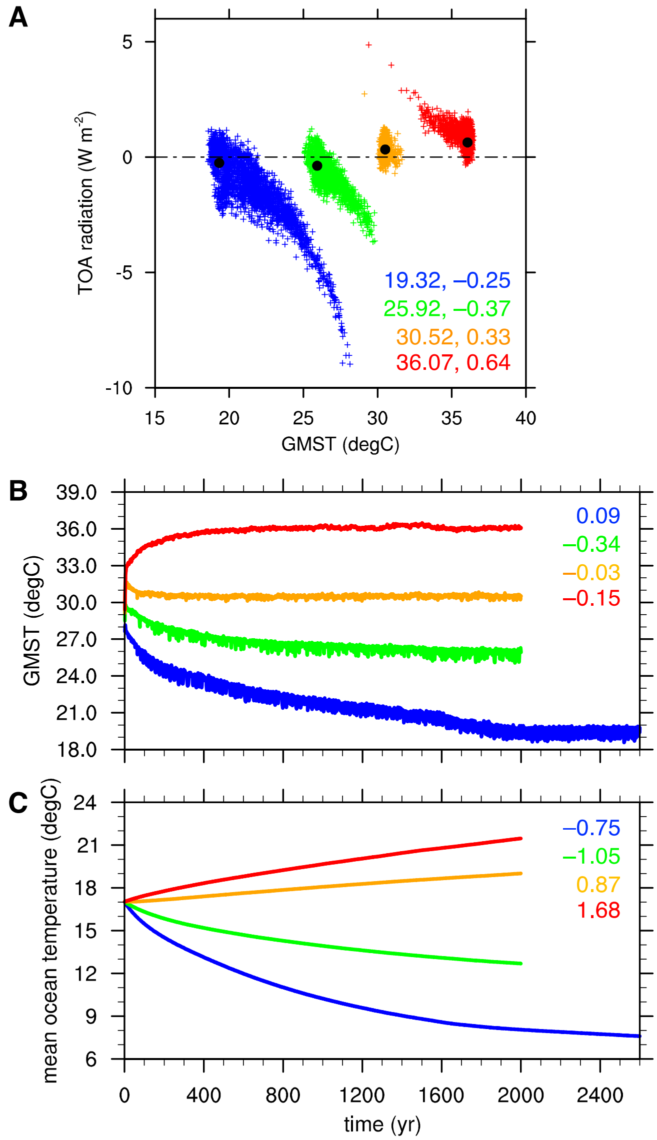

Fig. S2. Spin-up of the Eocene simulations. (**A**) Gregory plot, net radiation flux (in W m^{-2}) at top-of-atmosphere (TOA) versus global mean surface temperature (GMST; in ℃) in the Eocene 1× (blue), 3× (green), 6× (orange) and 9× (red) experiments. Black dots and color-coded numbers denote the average values over the last 500 years. (**B**) Time series of GMST the Eocene 1× (blue), 3× (green), 6× (orange) and 9× (red) experiments. (**C**) Time series of global mean ocean temperature for the Eocene 1× (blue), 3× (green), 6× (orange) and 9× (red) experiments. Color-coded numbers in (**B**) and (**C**) are the trend (in ℃ per 1000 years) over the last 500 years. The surface climate has reached quasi-equilibrium in all the simulations, but a substantial trend exists in deep ocean.

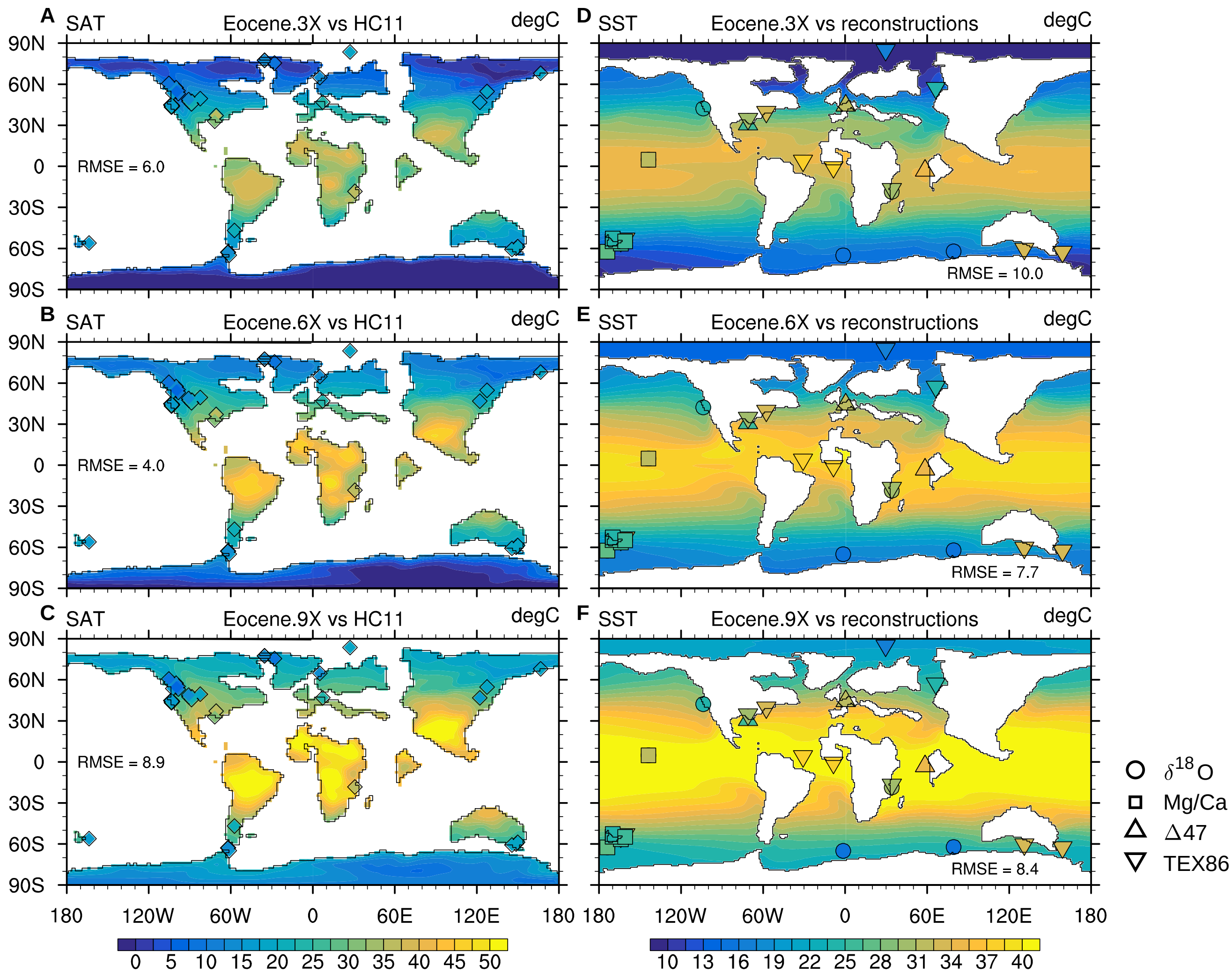

Fig. S3. Model-data comparison of Early Eocene surface temperature. (A) Surface air temperature (SAT; shading; in °C) in the Eocene 3× simulation compared with the terrestrial compilation of Huber and Caballero (HC11; diamonds) (*11*). **(B)** and **(C)**, As **(A)**, but for the Eocene 6× and 9× simulations. **(D)** Sea surface temperature (SST; shading; in °C) in the Eocene 3× simulation compared with published records for the early Eocene (markers; table S1). Inferred temperatures using $\delta^{18}O$ of planktic foraminifera, clumped isotopes, Mg/Ca of planktic foraminifera, and TEX_{86} are denoted as filled circles, upward-pointing triangles, squares and downward-pointing triangles, respectively. **(E)** and **(F)**, As **(D)**, but for temperature in the Eocene 6× and 9× simulations. Root mean square errors (RMSEs) of model results are listed. Note that the mean errors of proxies in HC11 and our SST compilation are approximately 3.4 °C and 6.4 °C, respectively.

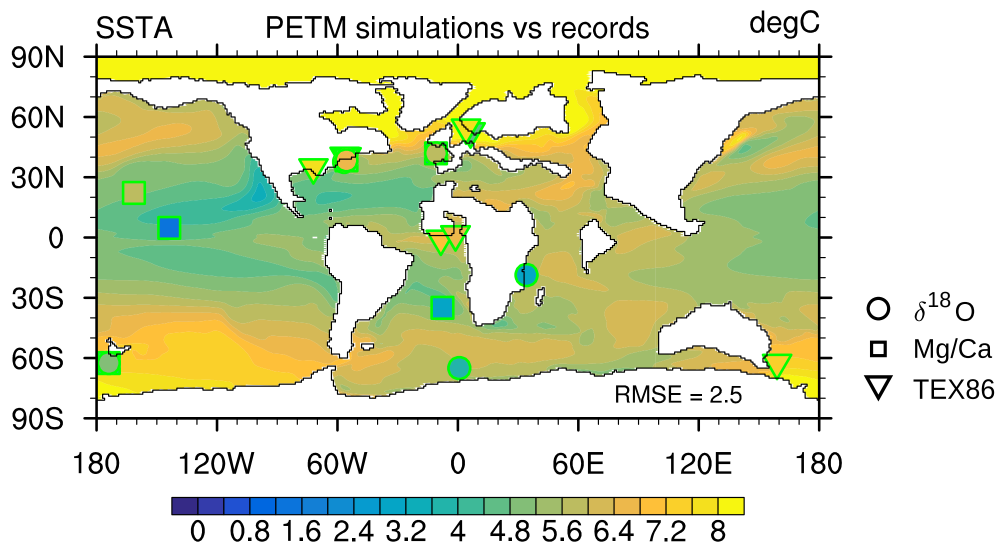

Fig. S4. Model-data comparison of PETM warming in SST. Anomalous sea surface temperature in Eocene simulations (SSTA; shading; in ℃) compared with proxy warming during the PETM (markers; table S2). Model SSTA are obtained by interpolating the Eocene simulations assuming a doubling CO_2 from a pre-PETM GMST of 27 ℃ (with a corresponding CO_2 of ~1140 ppmv). Reconstructions using $\delta^{18}O$ of planktic foraminifera, Mg/Ca of planktic foraminifera and TEX_{86} are denoted as filled circles, squares and downward-pointing triangles, respectively. Edge color of markers is coded green if a modeled PETM warming falls within proxy estimated range and otherwise red (table S2). Model simulations reproduce the PETM warming in all 21 proxy records within their uncertainties.

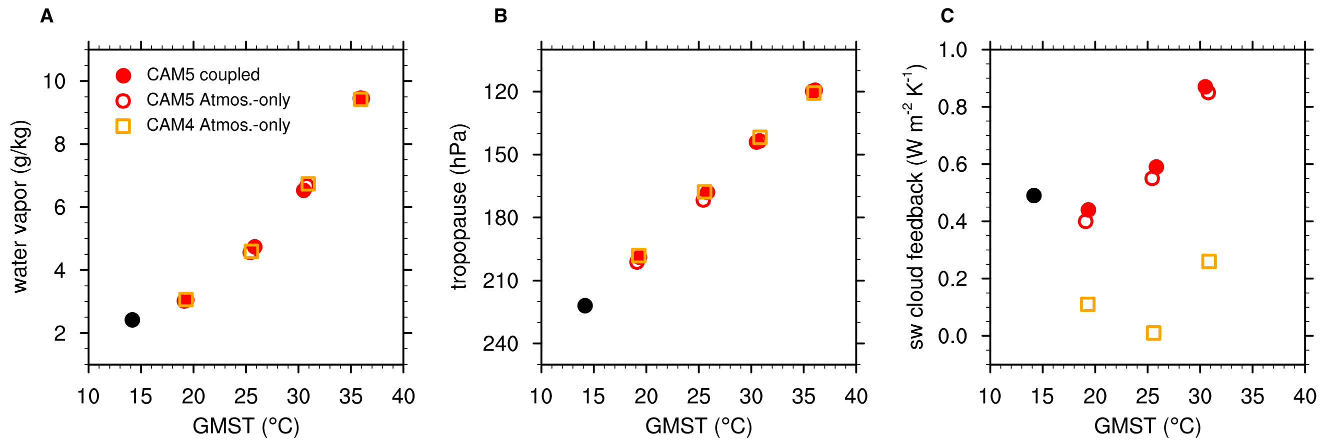

Fig. S5. Comparison of CAM5 and CAM4 Eocene atmosphere-only simulations. (A) Global mean water vapor content (in g kg^{-1}) in the atmosphere as a function of global mean surface temperature (GMST; in °C) in the atmosphere-only simulations using CAM5 (red circles) and CAM4 (orange squares). These atmosphere-only simulations are forced by the same sea surface conditions from the corresponding fully coupled Eocene simulations, as well as the same Eocene boundary conditions. For reference, global mean values in the fully coupled preindustrial (black filled circles) and Eocene simulations (red filled circles) are also plotted. **(B)** and **(C)**, As **(A)**, but for the tropical (30°S–30°N) mean tropopause pressure (in hPa) and the shortwave cloud feedback parameter (in W m^{-2} K^{-1}) calculated using the approximated partial radiative perturbation method. Water vapor and tropopause height change similarly with warming between CAM4 and CAM5, but the shortwave cloud feedback parameter is fundamentally different between models. The cloud shortwave feedback parameter in CAM4 simulations starts to increase with warming after exceeding a temperature threshold of ~25 °C. This threshold behavior broadly agrees with results in Caballero and Huber *(21)*, which exhibit a sharp rise of cloud feedback parameter at temperature above 23 °C.

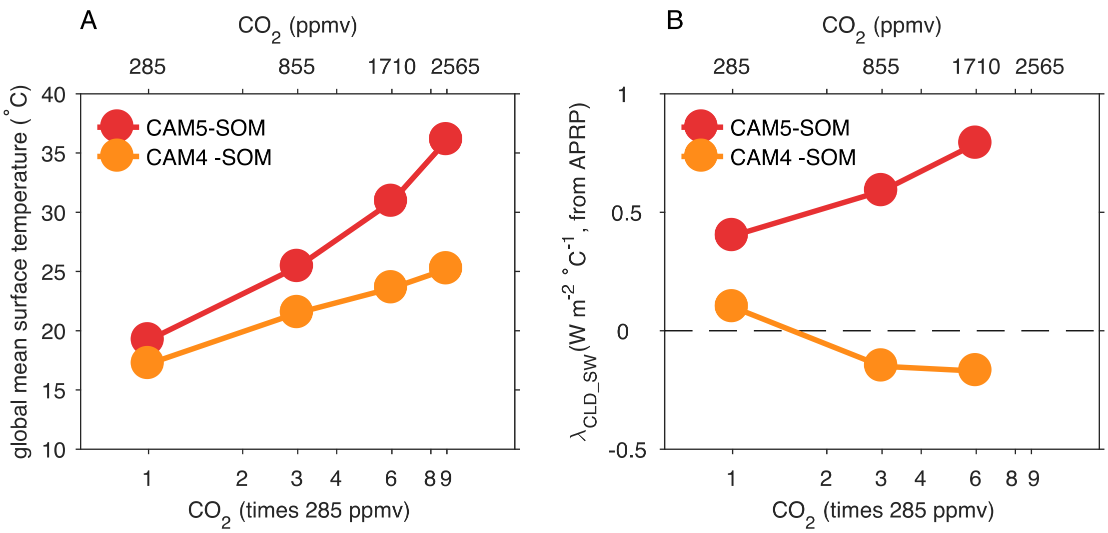

Fig. S6. Comparison of temperature and shortwave cloud feedback parameters between CAM5 and CAM4 Eocene SOM simulations. (A) Response of the global mean surface temperature (in °C) to increased atmospheric CO_2 concentration in CAM5 (red) and CAM4 (orange) simulations coupled to a slab ocean model (SOM). The same boundary conditions and diagnosed sea surface heat flux divergence and mixed layer depth from the corresponding fully coupled Eocene simulations are prescribed in the SOM simulations. **(B)** As **(A)**, but for the shortwave cloud feedback parameter (in W m^{-2} K^{-1}) calculated from the approximated partial radiative perturbation method. The same as the Eocene simulations coupled to a dynamic ocean, CAM5 with a slab ocean shows much higher climate sensitivity to CO_2 than CAM4, which is caused by the increasing shortwave cloud feedback parameter in CAM5 (versus slightly decreasing in CAM4). Climate sensitivity (slope in **(A)**) does not change much between CO_2 levels of 285–2565 ppmv (a GMST of 17.2–25.2 ℃) in CAM4 but increases substantially in CAM5.

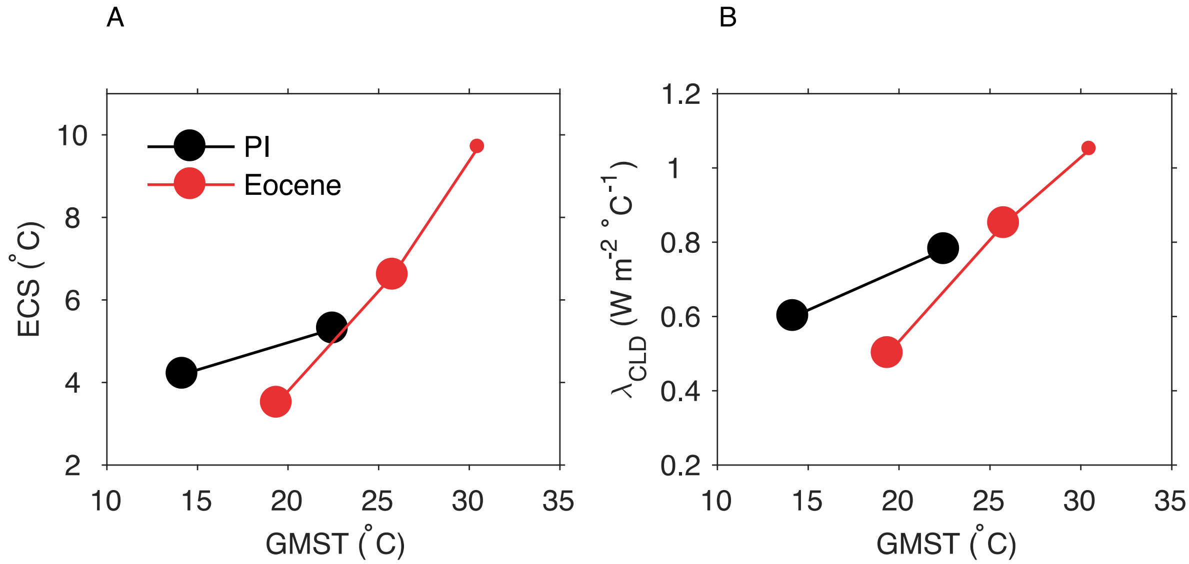

Fig. S7. Increase in climate sensitivity and cloud feedback parameter with warming under modern conditions. (A) Increase of ECS (in ℃) with warming under modern (black) and early Eocene conditions (red). **(B)** Increase of the cloud feedback parameter (in W m^{-2} K^{-1}) with warming under modern (black) and early Eocene conditions (red). ECSs and cloud feedback parameters based on modern boundary conditions for the preindustrial and a 4× CO_2 simulations are shown (Materials and Methods). ECSs and cloud feedback parameters based on the early Eocene boundary conditions include those from the Eocene 1×, 3× and 6× simulations. ECS and cloud feedback parameter for Eocene 6× are shown as a smaller marker than other Eocene simulations, as it is estimated from the 6× and 9× experiments, instead of using slab ocean simulations (Materials and Methods).

Table S1. Compilation of SST proxies for the Early Eocene. List of sites and proxy sea-surface temperature data used in this study including the core name, location, proxy type, mean early Eocene temperature (in ℃) and uncertainty (lower and upper errors). An Excel version of this table with references can be found in the Supplementary Materials.

Site	lon	lat	Paleo-lon	Paleo-lat	Type	SST	lower error	upper error
ODP 690B	1.20	-65.16	-1.35	-65.05	$\delta^{18}O$	15.5	2.3	2.3
Tanzania TDP3	39.63	-8.85	34.15	-18.65	$\delta^{18}O$	30.9	3.4	3.4
ODP 738	82.79	-62.71	79.40	-62.20	$\delta^{18}O$	16.0	0.9	0.9
DSDP 277	166.19	-52.22	-173.95	-62.45	$\delta^{18}O$	18.1	8.7	8.7
Mid-Waipara NZ	172.80	-43.04	-160.85	-54.85	$\delta^{18}O$	29.1	10.9	10.9
ODP 865	-179.56	18.44	-143.85	4.85	$\delta^{18}O$	28.1	2.1	2.1
Lodo Gulch	-120.64	36.59	103.75	42.25	$\delta^{18}O$	23.7	9.9	9.9
Mid-Waipara NZ	172.80	-43.04	-160.85	-54.85	Mg/Ca	26.3	4.7	4.7
ODP 865	-179.56	18.44	-143.85	4.85	Mg/Ca	32.5	4.7	4.7
Tawanui NZ	176.60	-39.90	-169.95	-52.75	Mg/Ca	24.2	4.7	4.7
Tora NZ	175.50	-41.50	-170.15	-54.75	Mg/Ca	26.2	4.7	4.7
Hampden Beach	170.80	-45.30	-164.05	-56.55	Mg/Ca	25.2	4.7	4.7
DSDP 277	166.19	-52.22	-173.95	-62.45	Mg/Ca	27.5	4.7	4.7
Mid-Waipara NZ	172.80	-43.04	-160.85	-54.85	TEX_{86}	33.5	8.4	8.6
Wilkes Land U1356A	136.00	-63.31	131.15	-62.35	TEX_{86}	33.8	8.3	5.7
South Dover Bridge	-76.00	38.60	-57.65	37.75	TEX_{86}	34.0	8.5	9.1
Western Siberian Seaway	73.52	53.50	66.35	55.25	TEX_{86}	24.4	5.2	6.4
ODP 1172	149.93	-43.96	159.00	-64.45	TEX_{86}	32.9	8.2	8.5
Hatchitigbee Bluff	-88.10	31.70	-71.05	32.65	TEX_{86}	30.7	7.8	7.8
Tanzania TDP3	39.63	-8.85	34.15	-18.65	TEX_{86}	31.0	8.3	7.7
ODP 929	-43.74	5.98	-30.80	2.10	TEX_{86}	37.5	9.4	11.6
Hampden Beach	170.80	-45.30	-164.05	-56.55	TEX_{86}	35.3	8.6	10.0
ACEX	134.18	87.87	29.60	82.95	TEX_{86}	17.5	5.6	4.9
ODP 959	-2.74	3.63	-8.55	-2.65	TEX_{86}	37.4	8.9	7.1
Hatchitigbee Bluff	-88.10	31.70	-71.05	32.65	$\Delta 47$	26.2	5.4	5.2
Kutch India K98.3	68.65	23.58	58.45	-1.15	$\Delta 47$	35.1	2.6	2.5
Egem Belgium EF2	3.90	50.90	0.45	46.45	$\Delta 47$	31.1	2.8	2.7
Egem Belgium EF1	3.90	50.90	0.45	46.45	$\Delta 47$	28.5	2.4	2.3
Kutch India K136.4	68.65	23.58	58.45	-1.15	$\Delta 47$	33.1	2.5	2.5
Kutch India K/N-06/5	68.65	23.58	58.45	-1.15	$\Delta 47$	30.4	2.5	2.4

Table S2. Compilation of SST proxies for the pre-PETM and PETM. List of sites and proxy sea-surface temperature data used in this study including the core name, location, proxy type, mean PETM and pre-PETM SST (in ℃) and uncertainty. An Excel version of this table with references can be found in the Supplementary Materials.

Site	Lon	Lat	Paleo-lon	Paleo-lat	Type	PETM SST	lower error	upper error	Pre-PETM SST	lower error	upper error
Bass River	-74.40	39.63	-55.55	38.45	$\delta^{18}O$	33.6	3.0	3.0	27.0	3.0	3.0
DSDP 277	166.19	-52.22	-173.95	-62.45	$\delta^{18}O$	21.9	8.7	8.7	16.8	8.7	8.7
ODP 865	-179.56	18.44	-143.85	4.85	$\delta^{18}O$	32.7	2.1	2.1	--	--	--
Tanzania TDP14	39.51	-9.28	34.15	-18.65	$\delta^{18}O$	33.3	3.4	3.4	30.1	3.4	3.4
Wilson Lake	-75.03	39.65	-56.45	38.65	$\delta^{18}O$	33.0	3.0	3.0	--	--	--
Nigeria SQ	3.60	6.80	-1.25	-0.45	$\delta^{18}O$	--	--	--	32.2	3.8	3.8
Lodo Gulch	-120.64	36.59	-103.75	42.25	$\delta^{18}O$	25.4	9.9	9.9	--	--	--
Tumey Gulch	-120.38	36.32	-102.85	41.15	$\delta^{18}O$	28	9.7	9.7	--	--	--
Milville	-75.08	39.39	-56.75	37.65	$\delta^{18}O$	33.2	3.0	3.0	29.3	3.0	3.0
ODP 689	3.10	-64.52	0.65	-65	$\delta^{18}O$	19.2	2.3	2.3	15.4	2.3	2.3
DSDP 401	-8.81	47.43	-10.95	41.95	$\delta^{18}O$	24.2	0.4	0.4	18.2	0.4	0.4
DSDP 549	-13.98	49.08	43.75	-15.65	$\delta^{18}O$	--	--	--	22.0	4.4	4.4
Bass River	-74.40	39.63	-55.55	38.45	Mg/Ca	26.3	4.7	4.7	21.5	4.7	4.7
DSDP 277	166.19	-52.22	-173.95	-62.45	Mg/Ca	31.0	4.7	4.7	27.4	4.7	4.7
DSDP 401	-8.81	47.43	-10.95	41.95	Mg/Ca	27.5	4.7	4.7	25.8	4.7	4.7
DSDP 527	1.76	-28.04	-7.75	-34.95	Mg/Ca	28.7	4.7	4.7	25.6	4.7	4.7
ODP 1209	158.51	32.65	-161.45	22.20	Mg/Ca	32.6	4.7	4.7	26.6	4.7	4.7
ODP 865	-179.56	18.44	-143.85	4.85	Mg/Ca	30.1	4.7	4.7	28.7	4.7	4.7
Nigeria SQ	3.60	6.80	-1.25	-0.45	Mg/Ca	--	--	--	30.3	4.7	4.7
ACEX	134.18	87.87	29.60	82.95	TEX_{86}	22.1	5.5	6.5	--	--	--
Bass River	-74.40	39.63	-55.55	38.45	TEX_{86}	37.3	8.5	7.2	30.2	7.6	4.7
Fur Section (North Sea)	9.10	56.80	4.05	52.65	TEX_{86}	29.2	5.1	7.0	17.7	6.1	4.9
Harrell Core	-88.72	32.25	-72.00	32.85	TEX_{86}	38.3	8.8	7.3	29.4	7.6	4.5
Nigeria IB10A	3.60	6.80	-1.25	-0.45	TEX_{86}	42.1	9.9	10.1	35.6	8.7	7.0
Nigeria IB10B	3.60	6.80	-1.25	-0.45	TEX_{86}	40.5	9.2	8.2	36.5	8.6	6.4
Nigeria SQ	3.60	6.80	-1.25	-0.45	TEX_{86}	--	--	--	36.4	8.7	7.0
ODP 1172	149.93	-43.96	159.00	-64.45	TEX_{86}	32.9	8.2	8.5	25.7	7.0	5.5
ODP 959	-2.74	3.63	-8.55	-2.65	TEX_{86}	43.1	9.9	9.0	36.2	8.7	6.6
Store Baelt Section (North Sea)	11.10	55.30	6.25	50.80	TEX_{86}	24.7	5.2	6.7	20.0	5.4	5.0
Mid-Waipara NZ	172.80	-43.04	-160.85	-54.85	TEX_{86}	36.5	8.8	10.6	--	--	--
Western Siberian Seaway	73.52	53.50	66.35	55.25	TEX_{86}	27.5	5.8	8.5	--	--	--
Wilson Lake	-75.03	39.65	-56.45	38.65	TEX_{86}	38.5	9.2	7.7	28.1	7.5	4.3

Table S3. Feedback analysis from the PRP calculations. Climate feedback parameters (in W m^{-2} K^{-1}) diagnosed from the two-way partial radiative perturbation method in the preindustrial and Eocene simulations. Values in parentheses are uncertainty calculated as the year-to-year standard deviation (N=4). Numbers in this table are used to generate Fig. 3B.

	PI	**1×**	**3×**	**6×**
cloud	0.60 (0.01)	0.50 (0.08)	0.85 (0.02)	1.05 (0.02)
(cloud SW)	0.47 (0.02)	0.37 (0.08)	0.63 (0.01)	0.88 (0.03)
(cloud LW)	0.13 (0.02)	0.13 (0.04)	0.22 (0.03)	0.17 (0.04)
water vapor	1.58 (0.02)	1.97 (0.03)	2.79 (0.02)	3.29 (0.02)
albedo	0.42 (0.04)	0.16 (0.01)	0.06 (0.01)	0.04 (0.00)
lapse rate	–0.30 (0.03)	–0.60 (0.07)	–1.04 (0.04)	–1.33 (0.07)
Planck	–2.81 (0.05)	–3.03 (0.03)	–3.37 (0.04)	–3.56 (0.02)